# *In situ* high temperature single crystal X-ray diffraction study of a natural omphacite

A. PAVESE[1,2,*], R. BOCCHIO[3] AND G. IVALDI[4]

[1] Dipartimento Scienze della Terra-Università degli Studi di Milano, Via Botticelli 23, 20133 Milano, Italy
[2] National Research Council, Centro di Studio per la geodinamica alpina e quaternaria, Via Botticelli 23, 20133 Milano, Italy
[3] Dipartimento Scienze della Terra-Università degli Studi di Milano, Via Botticelli 23, 20133 Milano, Italy
[4] Dipartimento Scienze Mineralogiche e Petrologiche-Università degli Studi di Torino, Via Valperga Caluso 35, 10125 Torino, Italy

### ABSTRACT

*In situ* high temperature single crystal X-ray diffraction (XRD) experiments have been performed on a chemically quasi-ideal omphacite sample $[(Ca_{0.49}Na_{0.51})_{\Sigma 1}(Mg_{0.46}Al_{0.48}Fe^{3+}_{0.06})_{\Sigma 1}(Si_{1.97}Al_{0.03})_{\Sigma 2}O_6]$, up to $1000°C$. The lattice parameters were studied as a function of temperature, and their thermal expansion coefficients determined. The *b* and *c* cell edges show discontinuities as a function of temperature which are interpreted here in terms of intracrystalline cation diffusion processes. Structure refinements have been carried out using data collected at room temperature, at $800°C$ and at ambient conditions after cooling. The structural behaviour as a function of temperature of chemically quasi-ideal omphacites is compared with those of jadeite and diopside.

KEYWORDS: omphacites, high temperature, thermal expansion.

## Introduction

OMPHACITES are aluminous pyroxenes with the ideal chemical formula $(Ca_{0.5}Na_{0.5})(Mg_{0.5}Al_{0.5})Si_2O_6$, and play an important role in high pressure-high temperature petrological processes, because of their wide thermobaric range of stability (Deer *et al.*, 1992). The asymmetric unit in *P2/n* omphacites comprises two tetrahedral sites (T1 and T2) which accommodate Si, two octahedral sites (M1 and M11) that host Mg and Al, two eightfold coordination sites (M2 and M21) over which Ca and Na distribute, and six oxygen atoms (labelling of sites according to Matsumoto *et al.*, 1975). Order-disorder (hereafter OD) reactions, activated by temperature, are well known to occur in omphacites, as a consequence of the partitioning of Mg, Al, Ca and Na cations, and cause a phase transition from the *P2/n* to *C2/c* space group. This transformation

was related to the occurrence of Anti-Phase-Domains, by Phakey and Ghose (1973) and by Carpenter (1980). Omphacites have been the subject of many a study devoted to investigate their crystal-chemistry (Clark and Papike, 1968; Matsumoto *et al.*, 1975; Aldridge *et al.*, 1978; Rossi *et al.*, 1983; Mottana *et al.*, 1997), the kinetics governing the OD reactions (Fleet *et al.*, 1978; Carpenter, 1981; Carpenter *et al.*, 1990*a,b*), the partitioning of $Fe^{2+}$ and $Fe^{3+}$, and its consequences (Camara *et al.*, 1998), the solid solution properties across the Di-Jd join (Carpenter and Smith, 1981), and the relationship between short-range and long-range order through single crystal XRD combined with infrared (IR) spectroscopy (Ballaran *et al.*, 1997, 1998*a,b*). Investigations aimed at providing insights into the microscopic mechanisms of ordering by means of theoretical modelling (Cohen, 1986; Davidson and Burton, 1987) have also been carried out.

Despite the central role played by omphacites in mineralogy, the knowledge of their high temperature behaviour relies upon inferences

\* E-mail: pavese@p8000.terra.unimi.it

from quenched samples only. This is because of the slow kinetics of transformation of these minerals at temperatures below 1000°C. However, *in situ* studies are the only way to investigate the behaviour of important structural observables.

In view of the above considerations, we undertook an *in situ* high temperature single crystal XRD study, conceived as a crystallographic investigation aimed at providing novel data on: (1) cell parameters *vs.* temperature. The detailed knowledge of the behaviour of lattice parameters *vs.* temperature and calculation of the thermal expansion coefficients contribute to the determination of the *P-V-T* equation of state which is fully defined as a function of a few thermoelastic coefficients, i.e. thermal expansion, bulk modulus and its first derivative *vs.* pressure (Vinet *et al.*, 1987; Pavese *et al.*, 1999*a*). (2) structural behaviour of omphacites upon heating, and comparison with earlier issues on diopside (Di) and jadeite (Jd), that have the *C*2/*c* space group.

## Experimental

### Sample

A single crystal of omphacite with prismatic shape (0.3 × 0.3 × 0.2 mm) from an eclogitic assemblage (Gorduno, Lepontine Alps, Switzerland; formation conditions estimated approximately *P* = 16 kbar and *T* = 720°C, after Bocchio *et al.*, 1985) was selected optically and used in the present study. The space group was confirmed as *P*2/*n*, by statistical analysis of collected reflections. Chemical analyses were performed using an ARL SEMQ electron-probe microanalyzer, in the wavelength-dispersive mode, and normalized to six oxygens p.f.u. The $Fe^{2+}$ and $Fe^{3+}$ contents were inferred following the method of Mottana (1986): (1) Ca and Na were constrained so as to fully occupy the M2 sites; (2) Mg and Al contents were re-scaled accordingly, and assumed to enter M1 sites; (3) the Fe content was determined as the residual to achieve full occupancy of the M1 sites, and partitioned into $Fe^{2+}$ and $Fe^{3+}$ in order to fulfil the electron neutrality principle. Titanium, which was also detected, occurred below the limits of reliable determination, and therefore was ignored. On this basis, we determined the composition as: $(Ca_{0.49}Na_{0.51})_{\Sigma 1}$ $(Mg_{0.46}Al_{0.48}Fe^{3+}_{0.06})_{\Sigma 1}(Si_{1.97}Al_{0.03})_{\Sigma 2}O_6$, which is very close to the ideal omphacite composition.

### Single crystal X-ray diffraction

Measurements were carried out using a Siemens P4 single-crystal X-ray diffractometer, with Mo-*K*α radiation. A resistance-heated $N_2$ flow (Argoud and Capponi, 1984) was used to heat the crystal, which was mounted on a quartz glass fibre positioned ~1 mm from the heater. A Pt-Rh thermocouple placed in the gas flow monitored the temperature and was calibrated to give a reading within ± 5°C of the true value. Temperature oscillations, during measurements, were maintained within ± 10°C. The data in this study were collected in three steps: (1) full data collection at room temperature and at 800°C for structure refinement purposes; both took approximately 10 days. In order to avoid cracks across the glue used to fix the crystal (caused by creep), and failure of the heater head, 800°C was the highest temperature which could be maintained for a full data collection. The HT equipment severely restricted the angular ranges of rotation of the diffractometer's axes, limiting the experimentally accessible regions of the reciprocal lattice; (2) determination of the cell parameters, from 25°C up to 1000°C, both on heating and cooling, using 25 reflections between 16 and 30°2θ. The highest temperature achieved was 1000°C. However, since this corresponds to the upper limit of the thermal range for which the heating device was calibrated, the actual highest *T* at the crystal was most probably 20−25°C lower than the set temperature. For these reasons data collected at 1000°C were ignored in the subsequent analysis, though they are plotted in Figs 1−2 for the sake of completeness; (3) full data collection at room temperature after cooling, to investigate transformations that occurred during the thermal treatment.

In Table 1 the instrumental conditions used to carry out the data collections are set out, along with the figures of merit of the structure refinements.

### Data treatment

Raw diffraction intensities were corrected for absorption by the semi-empirical Ψ-scan method of North *et al.* (1968). The structure refinements were carried out using two crystallographic software packages: GSAS (Larson and Von Dreele, 1987) and Siemens SHELXTL-PC. They produced results in agreement within ± 2σ. Here we report and discuss the results obtained using SHELXTL-PC. The atomic X-ray scattering

TABLE 1. Data collection parameters.

| | 25°C, before heating | 25°C, after cooling | 800°C |
|---|---|---|---|
| Tot. Refs. | 3610 | 3614 | 3263 |
| Unique. Refs. | 1732 | 1734 | 1697 |
| Peak width | | $1.6° + 0.1 \tan(\vartheta)$ | |
| $2\theta_{max}$ | 70° | 70° | 70° |
| $R$(Fo) | 0.034 | 0.038 | 0.040 |
| $wR$(Fo$^2$) | 0.12 | 0.13 | 0.14 |
| GOF | 1.3 | 1.3 | 1.2 |
| Ext. Coeff. | 0.044(3) | 0.039(3) | 0.048(5) |

curves from the database of SHELXTL-PC were used to compute the structure factors.

The anisotropic atomic displacement parameters, the atomic coordinates and the coefficient of secondary extinction $x$ [defined so as to multiply $F_c$ by $(1 + 0.001 \times x \times F_c^2 \times \lambda^3 / \sin(2\theta))^{-1/4}$] were refined, along with the occupancy factors of the M2 sites for Ca and Na cations. The M2 sites' occupancy factors were constrained in order to preserve the chemical composition and full site occupancy, requiring, therefore, the cation partitioning over M2 sites to formally depend on one degree of freedom only. Taking into account that (1) Mg and Al are difficult to distinguish by XRD, having similar scattering factors, and (2) our attempts to refine the occupancy factor of Fe on the M1 sites failed, providing results less significant than 3σ, we chose to partition Mg-Al-Fe equally over the M1 sites, and to maintain this distribution in the high temperature refinement also.

## Results and discussion

The thermal expansions of the lattice parameters and of the cell volume were determined by fitting linear functions to their temperature dependence. In the case of bond lengths, given that we have data available at ambient conditions (before and after the thermal cycle) and at 800°C only, expansivities were obtained from their difference. In the following we often use the generic term 'omphacites' implicitly meaning '$P2/n$-omphacites with quasi-ideal composition'.

### Lattice parameters

In Figs 1a,b,c and 2 the lattice parameters and the cell volume of omphacites are plotted as a

function of temperature, both upon heating and on cooling. In Table 2 their numerical values are reported. As general comments, we stress that: (1) although in most cases the cell parameters measured upon heating and on cooling agree with each other within the uncertainties, their trends as a function of $T$ exhibit slight discrepancies; (2) some lattice parameters, both upon heating and on cooling, show discontinuities, that, even if just significant at the ±1σ level, do not seem ascribable to statistical oscillations. However, such discontinuities have a negligible effect on the thermal expansion coefficients; (3) all refinements assumed $P2/n$ symmetry.

We interpret the lattice parameter variations set out in (1) and (2) in terms of the occurrence of intracrystalline diffusion processes and cation partitioning rearrangements, by analogy with similar behaviour of cell parameters observed in other minerals studied at high temperature, and affected by OD reactions (e.g Yamanaka and Takeuchi, 1983). Processes other than cation redistribution such as loss of Na by volatilization, exsolution of albite, formation of defects, were ruled out as (1) a search of extra peaks and (2) test refinements on tentative vacancy-bearing Na-deficient structures, using data collected at room temperature after the thermal cycle, failed to reveal any effect attributable to such reactions.

Let us comment on some features of the behaviour of the cell parameters as a function of temperature.

(1) Both $a^C$ and $a^H$ show smooth and quasi-linear trends (here and henceforth superscripts H and C refer to data obtained on heating or cooling, respectively) The thermal expansion coefficients, $\alpha_a^H$ and $\alpha_a^C$ (where $\alpha_X = 1/X \cdot dX/dT$) deviate from each other by ~7%. A 'bump' seems to occur at ~800°C, along $a^H$, but it is so slight an effect that it can not be distinguished unambiguously from noise. The values of $a^H$- and $a^C$ above 600°C practically coincide but exhibit increasing discrepancies on approaching room temperature, though they still remain within 3σ of each other. The $a$ lattice parameter thermal expansion coefficients of diopside and jadeite are 7.8 and $8.5 \times 10^{-6}°C^{-1}$, respectively (data from Cameron *et al.*, 1973) and their average ($<\alpha_a>$) is very close to $\alpha_a^H$, and not far from $\alpha_a^C$. This behaviour is in keeping with the fact that the $a$ lattice parameter is only modestly sensitive to the cation partitioning, and therefore it is intuitively expected to accord with the average composition, that in the case of ideal omphacites is 1/2Jd+1/2Di.
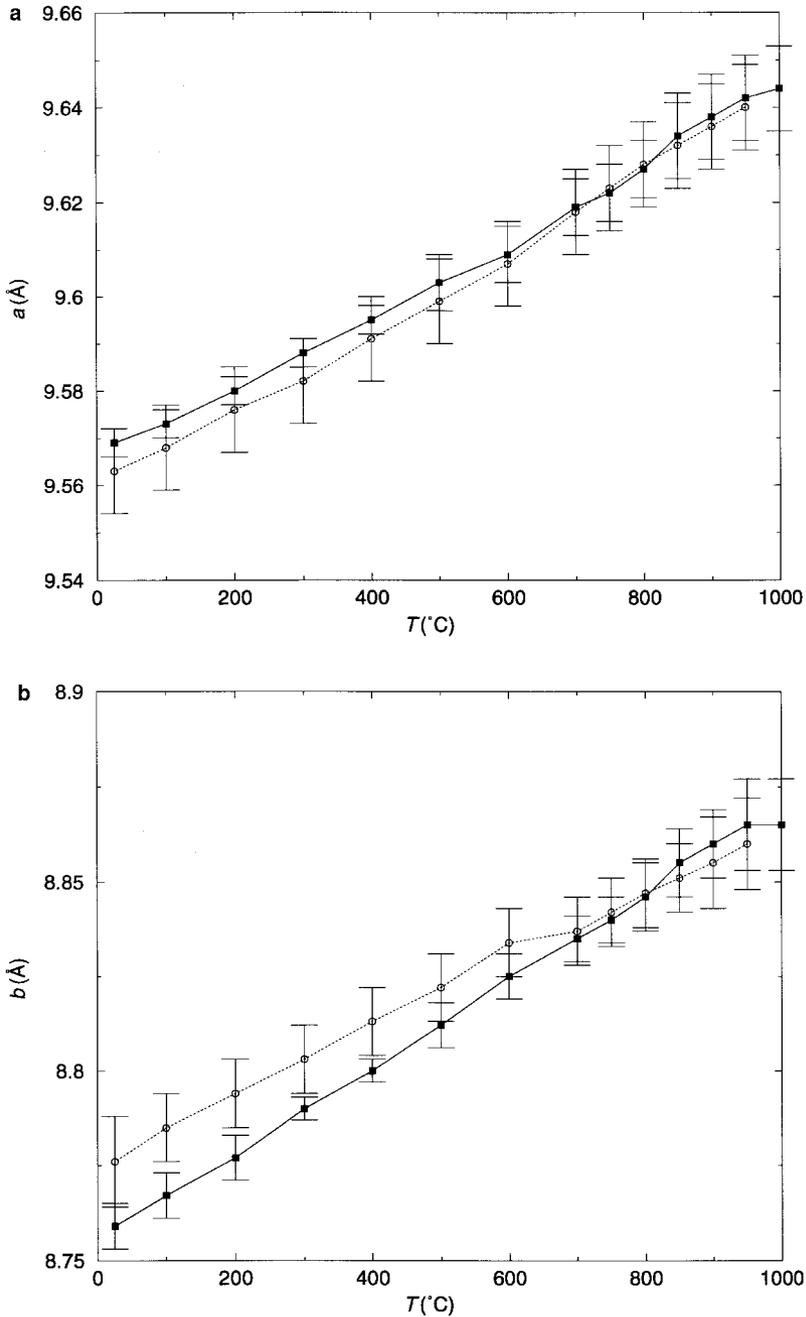
Fig. 1. (*a*) *a* lattice parameter (Å) as a function of temperature. Filled squares and empty circles correspond to measurements upon heating and on cooling, respectively. (*b*) *b* lattice parameter as a function of temperature. (*c*) (*opposite page*) *c* lattice parameter as a function of temperature. Symbols as in Fig. 1*a*.
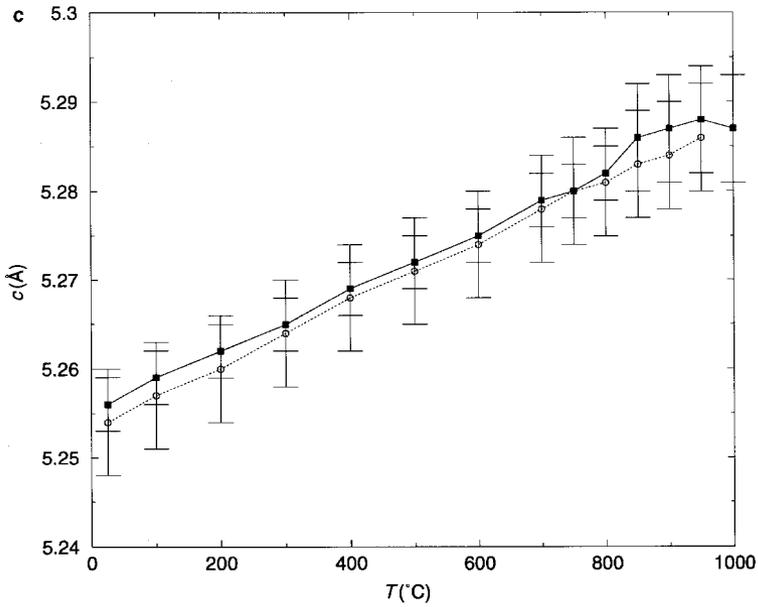
FIG. 1(*c*).

(2) The $b^H$ cell parameter exhibits a discontinuity as a function of temperature between 800 and 850°C. The relationship between $b$ and the array of M sites in omphacites is such that $b$ is expected to be the cell parameter most sensitive to cation rearrangements. The occurrence of a discontinuity
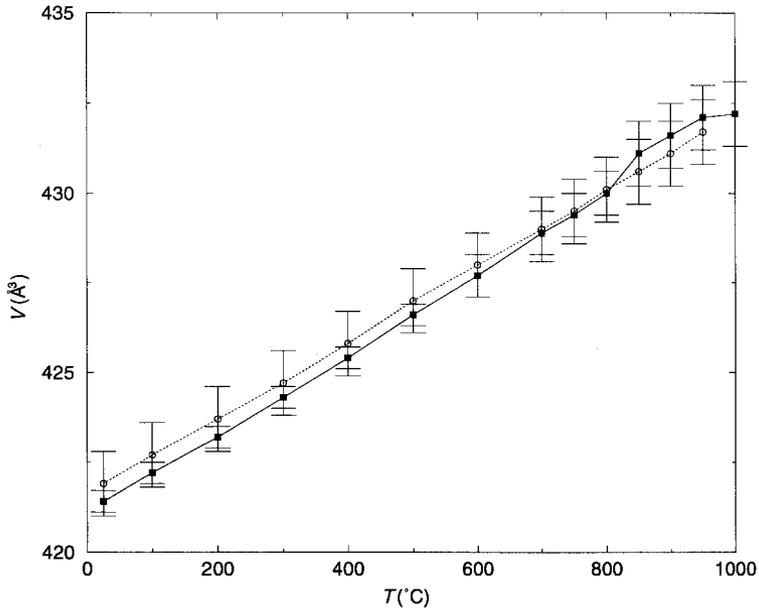


FIG. 2. Volume of the unit cell, $V$, ($\text{Å}^3$), as a function of temperature. Symbols as in Fig. 1*a*.

between 800 and 850°C is in keeping both with the estimate of the position of the $P2/n \rightleftharpoons C2/c$ transition given by Carpenter (1981), who suggests $T_c \approx 865°C$, and with the temperature of equilibration of the parent rock of our sample, estimated as $\approx 720°C$ but with a $100°C$ uncertainty. $b^C$ shows a discontinuity too, occurring between 600 and 700°C. $\alpha_b^H$ and $\alpha_b^C$ are ~24% apart. The inflections along $b^C$ and $b^H$ are shifted by ~200°C with respect to each other; this is possibly indicative of different cation distributions, giving rise to different thermoelastic behaviours in the crystal. Fe-oxidation processes are not thought to be responsible for these discontinuities, given that even if some ferrous iron was present in our crystal and underwent oxidation, it would be so modest that it should not give such substantial effects on the $b$ cell edge upon heating. In any case, this explanation cannot account for the discontinuity on cooling, and for $b$ being slightly larger at the end of the experiment than at the start. That is in contrast with the occurrence of the $Fe^{2+} \rightarrow Fe^{3+}$ oxidation reaction, entailing a shortening of $b$. Jd and Di have $\alpha_b$ equal to 10.0 and $20.5 \times 10^{-6°}C^{-1}$, respectively, with $\langle\alpha_b\rangle$ significantly larger than that of omphacite.

(3) The $c$ cell parameter, strictly related to the behaviour of the tetrahedral chain which responds to heating by kinking/straigthening, shows a discontinuity only upon heating between 800 and 850°C. This is consistent with the occurrence of the discontinuity observed on the $b$ cell parameter, and it seems reasonable to suppose it is due to the same effect. The thermal expansion coefficients $\alpha_c^H$ and $\alpha_c^C$ are in agreement with $\langle\alpha_c\rangle$, which is $6.4 \times 10^{-6°}C^{-1}$ (Jd and Di have 6.31 and $6.46 \times 10^{-6°}C^{-1}$, respectively).

(4) The cell volume (a) exhibits a discontinuity between 800 and 850°C upon heating, which is a consequence of those occurring on $c$ and $b$, and (b) shows a smooth curve on cooling. Jadeite and diopside have $\alpha_V = 24.7$ and $\alpha_V = 33.3 \times 10^{-6°}C^{-1}$, respectively, giving $\langle\alpha_V\rangle = 29 \times 10^{-6°}C^{-1}$, which compares with $\alpha_V^H = 27.6$ and $\alpha_V^C = 24.5 \times 10^{-6°}C^{-1}$.

The $\beta$ cell angle, which is sensitive to the OD configuration is reported in Table 2 but not discussed as its range of change, <0.1°, is too small with respect to the uncertainties, 0.03°, to provide reliable information.

Lastly, we observe that: (1) the relationship $\alpha_b > \alpha_a > \alpha_c$ shown by Cameron *et al.* (1973) is confirmed here for omphacites (using the average values of $\alpha_X = (\alpha_X^H + \alpha_X^C)/2$); and (2) the most apparent differences between the thermal expansion coefficients of Jd, Di and omphacites show up in the $b$ lattice parameter, in keeping with its sensitivity to the composition of the M sites. Whereas $\alpha_a$ and $\alpha_c$ are similar for Jd, Di and omphacite, $\alpha_b$ is markedly larger in Di.

## Structure

The contrast of atomic number between Na ($Z = 11$) and Ca ($Z = 20$) enabled us to carry out reliable refinements of Ca/Na occupancy at the M2 sites at high temperature. The results (Tables 3 and 4) indicate that at 800°C the occupancies of the M2 sites undergo change of the order of 0.01 atom per site. Although this value is comparable with the uncertainty, the slight increase towards disorder on the M2 sites is in keeping with the discontinuity observed above 800°C, affecting $b$ and $c$. The $Q_{M2}$ order parameter, computed according to Carpenter *et al.* (1990a), shows a shift from 0.42, before thermal treatment, to 0.38 after cooling, taking into account that $Q_{M1} \approx 2Q_{M2}$ (see Fig. 1 in Carpenter *et al.*, 1990a), $Q_{M1}$ moves from 0.84 to 0.76, i.e. towards more disordered Ca-Na and Mg-Al configurations, achieved at $T > 800°C$, and partly retained on cooling. The discontinuity of the $b^C$ curve between 600 and 700°C, in turn, might be due to the end of any exchange process. However, this inference is speculative and no direct evidence exists to support it.

The T1—O and T2—O tetrahedral bond lengths are essentially equal to each other, in agreement with our expectations from the chemical composition. The T sites exhibit very modest sensitivity to heating with slight changes affecting the third figure and of the same magnitude of the uncertainties. Upon heating the TILT1 and TILT2 angles (defined as the out-of-plane tilting angles, with respect to the tetrahedral basal oxygen atoms and (100) plane) which are sensitive to the cation partitioning over the M1 sites (Boffa Ballaran *et al.*, 1998), increase at similar rates, namely 0.0008 and 0.0007 degrees/°C, respectively. The O3—O3—O3 kink angle increases upon heating (as in Di and Jd (Cameron *et al*, 1973)), as the tetrahedral chain straightens, at a rate of 0.003 degrees/°C, against 0.0009 and 0.002 degrees/°C for Jd and Di, respectively. This suggests that the tetrahedral chain is more sensitive to heating in primitive (ordered) omphacites, than in C-centred Jd and Di. It is possible that crystal-chemical

TABLE 2. Lattice parameters (Å) and cell volume (Å$^3$) upon heating (upper set) and on cooling (lower set). Thermal expansion coefficients reported ($°C^{-1}$) are multiplied by $10^6$.

| $T(°C)$ | $a$ | $b$ | $c$ | $\beta$ | $V$ |
|---|---|---|---|---|---|
| 25 | 9.569(1) | 8.759(2) | 5.256(1) | 106.96(3) | 421.4(1) |
| 100 | 9.573(1) | 8.767(2) | 5.259(1) | 106.97(3) | 422.2(1) |
| 200 | 9.580(1) | 8.777(2) | 5.262(1) | 106.98(3) | 423.2(1) |
| 300 | 9.588(1) | 8.790(2) | 5.265(1) | 107.00(3) | 424.3(1) |
| 400 | 9.595(1) | 8.800(2) | 5.269(1) | 107.01(3) | 425.4(1) |
| 500 | 9.603(2) | 8.812(2) | 5.272(1) | 107.02(3) | 426.6(1) |
| 600 | 9.609(2) | 8.825(2) | 5.275(1) | 107.03(3) | 427.7(2) |
| 700 | 9.619(2) | 8.835(2) | 5.279(1) | 107.05(3) | 428.9(2) |
| 750 | 9.622(2) | 8.840(2) | 5.280(1) | 107.05(3) | 429.4(2) |
| 800 | 9.627(2) | 8.846(2) | 5.282(1) | 107.06(3) | 430.0(2) |
| 850 | 9.634(3) | 8.855(3) | 5.286(2) | 107.05(3) | 431.1(3) |
| 900 | 9.638(3) | 8.680(3) | 5.287(2) | 107.05(3) | 531.6(3) |
| 950 | 9.642(3) | 8.865(4) | 5.288(2) | 107.06(3) | 432.1(3) |
| 1000 | 9.644(3) | 8.865(4) | 5.287(2) | 107.03(3) | 432.2(3) |
| $\alpha_X^H$ | 8.3(2) | 13.2(1) | 6.6(1) | | 27.6(4) |
| 950 | 9.640(3) | 8.860(4) | 5.286(2) | 107.03(3) | 431.7(3) |
| 900 | 9.636(3) | 8.855(4) | 5.284(2) | 107.03(3) | 431.1(3) |
| 850 | 9.632(3) | 8.851(4) | 5.283(2) | 107.02(3) | 430.1(3) |
| 800 | 9.628(3) | 8.847(3) | 5.281(2) | 107.02(3) | 430.1(3) |
| 750 | 9.623(3) | 8.842(3) | 5.280(1) | 107.02(3) | 429.5(3) |
| 700 | 9.618(3) | 8.837(3) | 5.278(2) | 107.01(3) | 429.0(3) |
| 600 | 9.607(3) | 8.834(3) | 5.274(2) | 107.00(3) | 428.0(3) |
| 500 | 9.599(3) | 8.822(3) | 5.271(2) | 106.98(3) | 427.0(3) |
| 400 | 9.591(3) | 8.813(3) | 5.268(2) | 106.96(3) | 425.8(3) |
| 300 | 9.582(3) | 8.803(3) | 5.264(2) | 106.96(3) | 424.7(3) |
| 200 | 9.576(3) | 8.794(3) | 5.260(2) | 106.94(3) | 423.7(3) |
| 100 | 9.568(3) | 8.785(3) | 5.257(2) | 106.91(3) | 422.7(3) |
| 25 | 9.563(3) | 8.776(4) | 5.254(2) | 106.90(3) | 421.9(3) |
| $\alpha_X^C$ | 8.9(2) | 10.3(2) | 6.5(1) | | 25.1(3) |

effects due to cation partitioning add to those of barely thermal origin, which are generally dominant (Pavese *et al.*, 1999*b*), thus causing a larger O3—O3—O3 angle increase in omphacite than in Jd and Di.

The thermal expansivities of the average bond lengths at M1 and M11, $\alpha_{<M1-O>}$ and $\alpha_{<M1-O>}$, are 13.7 and $8.0 \times 10^{-6} °C^{-1}$, respectively; these values are close to $\alpha_{<M11-O>}$ for Di and Jd, which are 14.4 and $9.5 \times 10^{-6} °C^{-1}$, respectively. The behaviour of the M1 and M11 sites upon temperature is consistent with the fact that <M11—O> is shorter than <M1—O>, and hence the bond strengths of the M11—O bonds are greater than those of M1—O. Therefore the former is less sensitive to heating than the latter. A comparison between the thermal expansion

coefficients and the cation–oxygen bond lengths of the M1 and M11 sites in omphacites, and of the M1 sites in Jd and Di, suggests that Al may enter M11 in preference to M1. Di and Jd are reported to have <M2—O> thermal expansion coefficients as large as 16.4 and $12.8 \times 10^{-6} °C^{-1}$, respectively; these values are to be compared with $\alpha_{<M21-O>} = 14.9 \times 10^{-6} °C^{-1}$, and $\alpha_{<M2-O>} = 11.5 \times 10^{-6} °C^{-1}$, from the present study. This indicates that (1) values of $\alpha_{<M2X-O>}$ are qualitatively consistent with the Ca/Na cation partitioning observed, using as references the thermal expansion coefficients of sites fully occupied by Ca (Di) or Na (Jd); and that (2) in omphacites the M1 and M2 sites exhibit, on the whole, smaller thermal expansion than the corresponding sites with similar composition in

TABLE 3. Refined structural parameters of omphacite at room temperature, high temperature and room temperature after cooling (first (upper), second and third rows, respectively). U-equivalent displacement parameters are reported. Anisotropic displacement parameters and tables of structure factors are available from the Editor.

| | $x$ | $y$ | $z$ | Ueq. | Ca-occup. |
|---|---|---|---|---|---|
| T1 | 0.03948(5) | 0.84770(5) | 0.22674(8) | 0.0044(1) | |
| | 0.03918(6) | 0.84722(6) | 0.2258(1) | 0.0128(1) | |
| | 0.03924(6) | 0.84712(5) | 0.2269(1) | 0.0048(1) | |
| T2 | 0.03722(5) | 0.66247(5) | 0.73047(8) | 0.0043(1) | |
| | 0.03689(6) | 0.66333(6) | 0.7295(1) | 0.0130(1) | |
| | 0.03737(6) | 0.66177(5) | 0.7302(1) | 0.0047(1) | |
| M1 | 0.75 | 0.65926(8) | 0.25 | 0.0069(3) | |
| | 0.75 | 0.6578(1) | 0.25 | 0.0200(3) | |
| | 0.75 | 0.65870(9) | 0.25 | 0.0069(3) | |
| M11 | 0.75 | 0.84740(7) | 0.75 | 0.0033(2) | |
| | 0.75 | 0.8493(1) | 0.75 | 0.0138(3) | |
| | 0.75 | 0.84716(8) | 0.75 | 0.0039(3) | |
| M2 | 0.75 | 0.0523(1) | 0.25 | 0.0094(2) | 0.291(6) |
| | 0.75 | 0.0519(1) | 0.25 | 0.0310(4) | 0.303(9) |
| | 0.75 | 0.0522(1) | 0.25 | 0.0103(3) | 0.310(7) |
| M21 | 0.75 | 0.4505(1) | 0.75 | 0.0105(2) | 0.709(6) |
| | 0.75 | 0.4511(1) | 0.75 | 0.0340(3) | 0.697(9) |
| | 0.75 | 0.4501(1) | 0.75 | 0.0114(2) | 0.690(7) |
| O11 | 0.8630(1) | 0.8393(1) | 0.1201(2) | 0.0067(2) | |
| | 0.8635(2) | 0.8384(2) | 0.1196(3) | 0.0182(3) | |
| | 0.8628(1) | 0.8379(2) | 0.1215(3) | 0.0079(2) | |
| O12 | 0.8610(1) | 0.6780(1) | 0.6482(2) | 0.0067(3) | |
| | 0.8615(2) | 0.6789(2) | 0.6476(3) | 0.0184(3) | |
| | 0.8610(1) | 0.6770(2) | 0.6465(3) | 0.0079(2) | |
| O21 | 0.1149(1) | 0.0102(1) | 0.3093(2) | 0.0079(3) | |
| | 0.1145(2) | 0.0082(2) | 0.3058(3) | 0.0231(3) | |
| | 0.1142(2) | 0.0097(1) | 0.3086(3) | 0.0086(2) | |
| O22 | 0.1061(1) | 0.4975(1) | 0.8050(2) | 0.0090(2) | |
| | 0.1057(2) | 0.5002(2) | 0.8011(4) | 0.0264(4) | |
| | 0.1064(2) | 0.4970(1) | 0.8049(3) | 0.0095(2) | |
| O31 | 0.1066(1) | 0.7665(1) | 0.0039(2) | 0.0067(3) | |
| | 0.1053(2) | 0.7649(2) | 0.0046(3) | 0.0203(3) | |
| | 0.1060(1) | 0.7660(2) | 0.0039(2) | 0.0073(2) | |
| O32 | 0.0980(1) | 0.7403(1) | 0.4977(2) | 0.0071(3) | |
| | 0.0965(2) | 0.7428(2) | 0.4988(3) | 0.0206(3) | |
| | 0.0984(1) | 0.7399(2) | 0.4976(2) | 0.0074(2) | |

TABLE 4. Polyhedral volumes (Å$^3$), bond lengths (Å) and angles (deg), at room temperature before heating (25° BH), at high temperature (800°C) and at ambient conditions after cooling (25° AC). Average bond length thermal expansion coefficients (see text for definition), in °C$^{-1}$, are multiplied by 10$^6$.

| | 25° BH | 800°C | 25° AC | | 25° BH | 800°C | 25°A-C |
|---|---|---|---|---|---|---|---|
| T1—O21 | 1.597(1) | 1.598(2) | 1.599(2) | T2—O22 | 1.589(1) | 1.586(2) | 1.591(2) |
| O11 | 1.619(1) | 1.620(2) | 1.618(2) | O12 | 1.620(1) | 1.621(2) | 1.620(2) |
| O31 | 1.652(1) | 1.654(2) | 1.651(2) | O32 | 1.648(1) | 1.649(2) | 1.649(2) |
| O32 | 1.662(1) | 1.664(2) | 1.661(2) | O31 | 1.667(1) | 1.671(2) | 1.669(2) |
| Mean | 1.632(1) | 1.634(1) | 1.632(1) | Mean | 1.631(1) | 1.632(1) | 1.632(1) |
| O32-31-32 | 169.48 | 170.76 | 169.57 | | | | |
| TAV | 24.55 | 25.07 | 24.65 | | 21.77 | 22.66 | 21.64 |
| TQE | 1.0071 | 1.0059 | 1.0223 | | 1.0084 | 1.0063 | 1.0039 |
| TILT | 3.43 | 3.63 | 3.20 | | 1.87 | 2.09 | 1.76 |
| Volume | 2.21 | 2.22 | 2.20 | | 2.20 | 2.21 | 2.22 |
| M1—O22x2 | 2.024(1) | 2.044(2) | 2.017(2) | M11-O21x2 | 1.886(1) | 1.898(2) | 1.895(2) |
| O12x2 | 2.059(1) | 2.068(2) | 2.051(2) | O11x2 | 1.932(1) | 1.940(2) | 1.938(2) |
| O11x2 | 2.134(1) | 2.159(2) | 2.125(2) | O12x2 | 1.987(1) | 2.015(2) | 1.997(2) |
| Mean | 2.072(1) | 2.090(1) | 2.064(1) | Mean | 1.935(1) | 1.951(1) | 1.943(1) |
| $\alpha_{<x>}$ | | 13.7(5) | | | | 8.0(5) | |
| Volume | 11.57 | 11.93 | 11.49 | | 9.53 | 9.80 | 9.67 |
| M2—O11x2 | 2.355(1) | 2.383(2) | 2.363(2) | M21—O22x2 | 2.388(1) | 2.410(2) | 2.388(2) |
| O21x2 | 2.364(1) | 2.386(2) | 2.369(2) | O12x2 | 2.391(1) | 2.418(2) | 2.393(2) |
| O32x2 | 2.459(2) | 2.469(2) | 2.464(2) | O31x2 | 2.476(1) | 2.493(2) | 2.476(2) |
| O31x2 | 2.693(1) | 2.734(2) | 2.699(2) | O32x2 | 2.776(1) | 2.827(2) | 2.770(2) |
| Mean | 2.468(1) | 2.493(1) | 2.474(1) | Mean | 2.508(1) | 2.537(1) | 2.507(1) |
| $\alpha_{<x>}$ | | 9.5(5) | | | | 14.9(5) | |
| Volume | 24.53 | 25.35 | 24.97 | | 25.82 | 26.76 | 25.90 |

Jd and Di (i.e. Na-, Al-, Ca- or Mg-bearing) The second point might be explained, on crystal-chemical grounds, in terms of the fact that $P2/n$ omphacites have a larger number of structural degrees of freedom than the $C2/c$ end-members Jd and Di, and thus omphacite has greater potential for readjusting its cation geometries upon temperature change.

## Conclusions

On the basis of the results presented and discussed above, obtained from *in situ* high temperature single crystal XRD measurements, up to 1000°C, we draw the following conclusions.

The thermal expansion coefficients of the cell edges are: $\alpha_a^H = 8.3(2)$, $\alpha_a^C = 8.9(2)$, $\alpha_b^H = 13.2(1)$, $\alpha_b^C = 10.3(2)$, $\alpha_c^H = 6.6(1)$, $\alpha_c^H = 6.5(1)$, $\alpha_V^H = 27.6(4)$, $\alpha_V^C = 25.1(3) \times 10^{-6}°C^{-1}$. The discrepancies between $\alpha_b^H$ and $\alpha_b^C$ (24% apart) and the inflections revealed by some cell edges as a function of temperature are attributed to OD reactions. Omphacite, Jd and Di show similar thermal expansion along $a$ and $c$, but are different along $b$; we believe that this is indicative of the sensitivity of the $b$ cell parameter to the cations occupying the M1 sites.

The structure refinements at room temperature before the thermal cycle, at 800°C and at ambient temperatures after cooling, show: (1) the tetrahedral chains respond to heating by straightening (increasing of the O3—O3—O3 angle), and by increasing the out-of-plane tilting angles; (2) smaller thermal expansion coefficients of the cation–oxygen bond length for the M11(M2) sites than for the M1(M21) sites, in keeping with <M11—O>(<M2—O>) being shorter than <M1—O>(<M21—O>), see Table 4; (3) lower sensitivity to heating for the M-sites in omphacites than for the corresponding sites with similar composition in Jd and Di (i.e. Na-, Al-, Ca- or Mg-bearing).

## Acknowledgements

## References

Aldridge, L.P., Bancroft, G.M., Fleet, M.E. and Herzberg, C.T. (1978) Omphacite studies, II. Mössbauer spectra of C2/c and P2/n omphacites. *Amer. Mineral.*, **63**, 1107−15.

Argoud, R. and Capponi, J.J. (1984) Soufflette a haute temperature pour l'etude de monocristaux aux rayons X et aux neutrons jusqu'a 1400 K. *J. Appl. Crystallogr.*, **17**, 420−5.

Bocchio, R., Liborio, G. and Mottana, A. (1985) Petrology of the amphibolitized eclogites of Gorduno, Lepontine Alps, Switzerland. *Chem. Geol.*, **50**, 65−86.

Boffa Ballaran, T., Carpenter, M.A., Domeneghetti, M.C. and Tazzoli, V. (1997) Hard mode infrared spectroscopy of cation ordering and substitution in a chain silicate. *Phase Transitions*, **63B**, 159−70.

Boffa Ballaran, T., Carpenter, M.A., Domeneghetti, M.C. and Tazzoli, V. (1998a) Structural mechanisms of solid solution and cation ordering in augite-jadeite pyroxenes: I. A macroscopic perspective. *Amer. Mineral.*, **83**, 419−33.

Boffa Ballaran, T., Carpenter, M.A., Domeneghetti, M.C., Salje, E.K.H. and Tazzoli, V. (1998b) Structural mechanisms of solid solution and cation ordering in augite-jadeite pyroxenes: II. A microscopic perspective. *Amer. Mineral.*, **83**, 434−50.

Camara, F., Nieto, F. and Oberti, R. (1998) Effects of $Fe^{2+}$ and $Fe^{3+}$ contents on cation ordering in omphacite. *Eur. J. Mineral.*, **10**, 889−906.

Cameron, M., Sueno, S., Prewitt, C.T. and Papike, J.J. (1973) High-temperature crystal chemistry of acmite, diopside, hedenbergite, jadeite, spodumene, and ureyite. *Amer. Mineral.*, **58**, 594−618.

Carpenter, M.A. (1980) Mechanisms of exsolution in sodic pyroxenes. *Contrib. Mineral. Petrol.*, **71**, 289−300.

Carpenter, M.A. (1981) Time-Temperature-Transformation (TTT) analysis of cation disordering in omphacite. *Contrib. Mineral. Petrol.*, **78**, 433−40.

Carpenter, M.A. and Smith, D.C. (1981) Solid solution and cation ordering limits in high temperature sodic pyroxenes from the Nybö eclogite pod, Norway. *Mineral. Mag.*, **44**, 37−44.

Carpenter, M.A., Domeneghetti, M.C. and Tazzoli, V.

(1990a) Application of Landau theory to cation ordering in omphacite I: equilibrium behaviour. *Eur. J. Mineral.*, **2**, 7−18.

Carpenter, M.A., Domeneghetti, M.C. and Tazzoli, V. (1990b) Application of Landau theory to cation ordering in omphacite II: kinetic behaviour. *Eur. J. Mineral.*, **2**, 19−28.

Carpenter, M.A., Powell, R. and Salje, E. (1994) Thermodynamics of non-convergent ordering in minerals: I. An alternative approach. *Amer. Mineral.*, **79**, 1053−67.

Clark, J.R. and Papike, J.J. (1968) Crystal-chemical characterization of omphacites. *Amer. Mineral.*, **53**, 840−68.

Cohen, R.E. (1986) Configurational thermodynamics of aluminous pyroxenes: a generalized pair approximation. *Phys. Chem. Min.*, **13**, 183−97.

Davidson, P.M. and Burton, B.P. (1987) Order-disorder in omphacitic pyroxenes: a model for coupled substitution in the point approximation. *Amer. Mineral.*, **72**, 337−44.

Deer, W.A., Howie, R.A. and Zussman, J. (1992) *An Introduction to the Rock-forming Minerals*. John Wiley and Sons, New York.

Fleet, M.E., Herzberg, C.T., Bancroft, G.M. and Aldridge, L.P. (1978) Omphacite studies, I. The $P2/n \rightarrow C2/c$ transformation. *Amer. Mineral.*, **63**, 1100−6.

Larson, A.C. and Von Dreele, R.B. (1987) *GSAS: General Structure Analysis System*. Los Alamos National Laboratory, Report LAUR:86-87.

Matsumoto, T., Tokonami, M. and Morimoto, N. (1975) The crystal structure of omphacite. *Amer. Mineral.*, **60**, 634−41.

Mottana, A. (1986) Crystal-chemical evaluation of garnet and omphacite microprobe analyses: its bearing on the classification of eclogites. *Lithos*, **19**, 171−86.

Mottana, A., Murata, T., Wu, Z.Y., Marceli, A. and Paris, E. (1997) The local structure of Ca-Na pyroxenes. 1. XANES at the Na K-edge. *Phys. Chem. Min.*, **24**, 500−9.

North, A.C.T., Phillips, D.C. and Mathews, F.S. (1968) A semi-empirical method of absorption correction. *Acta Crystallogr.*, A**24**, 351−9.

Pavese, A., Ferraris, G., Pischedda, V. and Mezouar, M. (1999a) Synchrotron powder diffraction study of phengite 3T from the Dora Maira massif: p-V-T equation of state and petrological consequences. *Phys. Chem. Min.*, **26**, 460−7.

Pavese, A., Ferraris, G., Pischedda, V. and Ibberson, R. (1999b) Tetrahedral order in phengite $2M_1$ upon heating, from powder neutron diffraction, and thermodynamic consequences. *Eur. J. Miner.*, **11**, 309−20.

Phakey, P.P. and Ghose, S. (1973) Direct observation of

anti-phase domain structure in omphacite. *Contrib. Mineral. Petrol.*, **39**, 239−45.

Rossi, G., Smith, D.C., Ungaretti, L. and Domeneghetti, M.C. (1983) Crystal-chemistry and cation ordering in the system diopside-jadeite: a detailed study by crystal structure refinement. *Contrib. Mineral. Petrol.*, **83**, 247−58.

Vinet, P., Smith, J.R. and Rose, J.H. (1987) Temperature effects on the universal equation of state of solids. *Phys. Rev. B*, **35**, 1945−53.

Yamanaka, T. and Takeuchi, Y. (1983) Order-disorder transition in $MgAl_2O_4$ spinel at high temperature up to 1700°C. *Zeits. Kristallogr.*, **165**, 65−78.